Numerical Model of a Planar Jet Wiping System for Continuous Strip Lines

Celia Miguel-González[1], Manuel García-Díaz[1], Bruno Pereiras[1], Miguel Vigil[2] and Alejandro Rodríguez de Castro[3]

[1]University of Oviedo, Energy Department, Campus de Viesques, 33271, Gijón, Spain, [2]University of Oviedo, Project Engineering Area, Calle Independencia 13, 33004, Oviedo, Spain,[3]ArcelorMittal Global R&D Asturias, P.O. Box 90, 33400, Avilés, Spain

(Received 000 0, 2020; Revised 000 0, 2020; Accepted 000 0, 2020)

Keywords: CFD; Wiping; Steel strip; Air-Knife; Tinning line.

Correspondence to: Celia Miguel-González

Abstract

The present study focuses on the numerical modelling of gas-jet wiping process. Many processes involving liquids are necessary during steel manufacturing, such as cooling, lubrication or cleaning. Satisfactory processes for removing the liquid are critical for the quality of the product obtained as well as for avoiding a product rejection in strip lines such as tandem mills and tinning lines. One the most widespread drying technology used is based on planar air-knives or nozzle rows which wipe the liquid out from the steel strip by creating an aerodynamic barrier.

The objective of this paper is to analyze the performance of a simple air knife based on an inclined planar jet that is commonly used in many commercial or in-house built devices. A CFD model developed by using commercial software ANSYS FLUENT® was built in order to evaluate the wiping system depending on the type of feeding: central and lateral.

1. Introduction

Many processes involving liquids are necessary during steel manufacturing, such as water cooling, lubrication, or cleaning. However, once those liquids have accomplished their purpose, they must be removed from the product surface because unsatisfactory drying critically affects downstream the production process and it would lead into a high degree of product rejection. Therefore, drying the product after the application of these fluids is completely critical for the whole performance of a steel manufacturing line in order to boost the productivity.

Cold rolling mills or continuous coating lines are, for example, facilities where drying a continuous strip is a bottleneck in the productivity because new advances in technology, such as improved lubrication, process control, rolling techniques, etc., have noticeably increased the speed of the lines. The objective of the cold rolling mills, which is tandem or temper mill, is to reach the final thickness, metallurgical qualities and to get better surface quality and metallurgical homogeneity of the coils. To do this, they used to work in wetted conditions usually employing a water-based emulsion which is critical for the quality of the product. This emulsion must be removed from the product before coiling in order to avoid stains.

On the other hand, in tinplate lines the strip passes through a rinsing tank that covers it with an aqueous solution before the application of coating. The objective of these lines is to provide the steel substrate of a tin coating for its electrochemical protection and set down a passivation layer that protects its surface during storage. In turn, this passivation layer constitutes a suitable anchor for lacquers and varnishes.

Drying technologies have been in the spotlight in the last decades in many fields: food industry, minerals, etc… A good review of these techniques can be seen in [1]. Nevertheless, it is known that drying is not the best solution in many processes where optical equipment is used for measurement or process control, for example in the case of steel industry. The steam generated during a drying process could hinder the performance of optical measurement devices, or even damage them [2].

Therefore, other technologies commonly based on mechanical and/or aerodynamic principles should be used. Many patents related to drying systems for steel industry may be found, and many industrial suppliers offer their equipment. Despite the existence of hybrids systems, a large percentage of commercial devices are based only on aerodynamics: air knives, air nozzle rows, vacuum-aid systems, etc., are employed to remove the liquid from the surface. These kinds of systems are also applied in food industry, electronics, pharmaceutical, etc. where particle deposits, both liquid and solid, can damage the final product. The key, in the case of steel industry, is the amount of liquid to be removed. As an example, in cold rolling the 95% of the electricity consumed is transformed into heat in the roll bite. A standard tandem mill of 5 stands consuming from 15 to 20MW/h needs about 1000 m^3/h of refrigeration water flow. Another example is the tinning line within the rinsing section, where the strip, due to its own process inertia speed (which can reach 500 m/min), drags a layer of water (up to 10 microns). It is critical to

remove all the residual humidity left after the rinsing section and before applying the passivation solution.

The most basic system for blowing-off liquid from a surface is an impinging round jet, perpendicular or oblique to the strip. The phenomena associated to an impingement round jet has been extensively studied by several authors using analytical, experimental and Computational Fluid Dynamics (CFD) techniques. All the work related to this topic mention two separated regions: the impingement jet and the axisymmetric wall jet generated downstream the stagnation point (see Fig. 1, A). The wall jet resulting from an axisymmetric round jet has been experimentally studied in [3]. In [4], it was presented experimental measurements about the wall jet of a round jet impinging orthogonally on a flat surface using hot-wire anemometry. CFD techniques are also used for research on round jets. In [5], it is presented a numerical study of a round jet impinging normally onto a liquid surface and the results obtained were compared with Particle Image Velocimetry (PIV) measurements. And in [6], CFD is used to calculate the velocity fields of impinging jets. Moreover, there are some references ([7], [8]) where correlations to assess the velocity profile of such wall jets can be found, both laminar and turbulent flow which is defined by Reynolds number at jet exit. Industrial applications of round jets to blow off liquids on surfaces can be found in [5], [8] and [9].

However, arrays of round jets do not provide optimum blowing conditions for continuous strip lines and it is not common to see arrays of round jets in such installations. This ground is more propitious to planar jets, whose interaction with planar surfaces has been also analyzed from different points of view [11]–[13]. It is important to remark that while for normal impingement of planar jets the flow is entirely symmetric, this is not for oblique impingement as can be seen in Fig. 1 B, where D is the gap of the nozzle, U_o is the mean velocity through the nozzle outlet, H is the distance of blowing, U_m is the maximum velocity of the wall jet, δ is the boundary layer thickness and τ is the wall shear stress. The wall shear stress is an important factor for wiping. It is known that, in coating lines, the wall shear stress (τ) has a significant effect on the wiping results [14]. In [15] it is demonstrated that the final coating thickness depends on both pressure at the stagnation region and shear stress caused by the wall jet. Therefore, it can be easily concluded that shear stress will have a main role in drying systems based on aerodynamic wiping.

Nonetheless, bibliography about planar jets wiping liquids on planar surfaces is scarce. Most of it deals with the performance of air knives in Hot Dip Galvanizing (HDG) lines, where the planar jet created by the air knives is used to wipe the excess of molten zinc [16]. This topic has been exhaustively studied through the last decades using a wide range of techniques. In [17], it is presented a CFD aerodynamic study of an air-knife for galvanizing process in order to find out the causes of the check mark. In [18], it is presented a study of a jet-wiping interaction for galvanization process in order to evaluate the splashing phenomena. [11] also studies the process by means of two-phase numerical simulations and compare different types of turbulence models. And a numerical analysis in order to predict the sag line formation and the coating thickness is presented in [19].

Unfortunately, work related to the utilization of planar jets with the aim of blowing-off liquids from a continuous strip is really limited due to the complexity of the problem because it involves an extremely thin liquid layer combined with a very large domain. Nevertheless, since the liquid layer is very thin, its effects on the wall jet could be considered negligible.

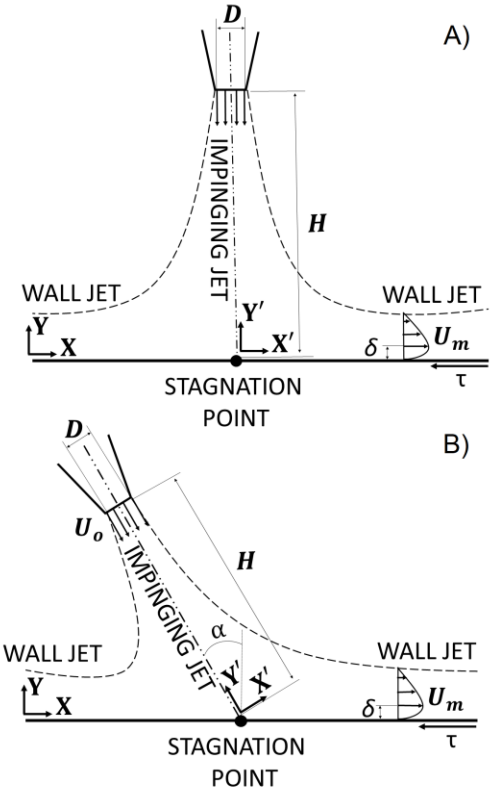

Fig. 1. A: Axisymmetric round jet or planar impinging perpendicularly on a planar surface. B: inclined planar jet impinging on a planar surface.

In this work the authors analyze the performance of a single planar jet, working as an air knife, which is present in many commercial or in-house built devices. Commercial systems supplied by manufacturers do not present flaws generally, but many times, these systems must be installed in previously built factories which need to improve the drying process. In these cases, it is common to face a real problem about finding enough space to install such devices, thus, changes on the mechanical design of the systems could be needed. Those changes could deteriorate the performance, even finding that no improvement was achieved after installing the new device, which is generally very expensive. This work is focused on the study of an air knife that was modified for its installation in a tin-plate line. The mechanical design was changed to allow the feeding air to enter from the top of the air knife instead of from the side (Fig. 2). Apart from that, the width of the air knife slot is set by using an array of screws. Due to the proximity of the air knife to the strip surface, the effect of the wake of these screws on the pressure and velocity fields has been analyzed.

The study is based on the application of CFD techniques to assess the pressure and velocity field. The numerical model has been validated using data from the bibliography. The analysis of the results has shown that the position of the inlet

critically affects the performance of the system as it will be shown afterwards.

2. Material and Methods

In this section the authors describe the numerical model employed. The details of the geometry, the building of the mesh and the characteristics of the numerical model are exposed in the following subsections.

2.1 Geometry

The geometry of the model is composed of an air knife (Fig. 2), which gap (*D*, see Fig. 1) is 24mm, blowing onto a strip 25 mm (*H*, see Fig. 1).

In order to perform the study of different configurations of the collector, lateral/central feeding and screws influence, a geometry that includes all the possibilities was generated with the aim of simplify the mesh generation process. When the lateral feeding is simulated, the central feeding is disabled and vice versa.

The air-knife width is 1400 mm, and the strip width (*Z*) is 1200 mm. According to the manufacturer's specifications, the planar jet should be blowing with a deviation of 10˚ - 15˚ (*α* in Fig. 1) from perpendicular to the strip and against the direction of the strip velocity. The analysis was performed with an air-knife located at an angle of 10˚.

There are 12 screws (see Fig. 2, C) in the air-knife but only 10 of them are located over the 1200 mm of strip. The screws have a diameter of 5 mm, which is a fifth part of the gap between the air-knife and the strip. The first and last screw holes are separated L_2=30 mm from the sides of the air-knife, whereas the whole set is placed in a regular pattern separated L_3=121 mm from each other.

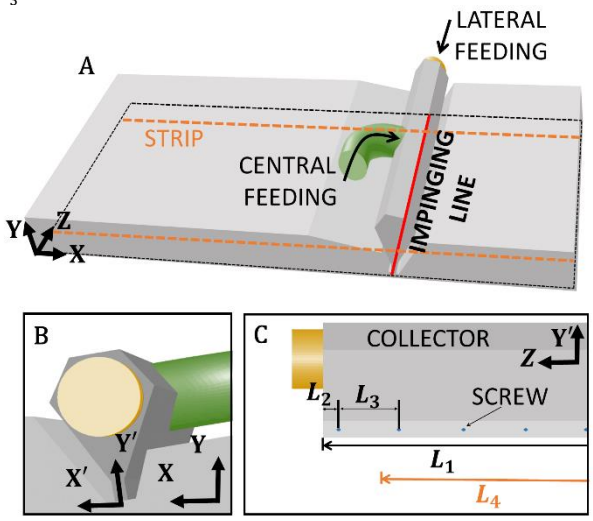

Fig. 2. A) Sketch of the geometry of the model. B) Detail of the lateral feeding. C) Detail of the collector: collector width L_1=1400 mm, separation of the first and last screw from the side L_2=30 mm, separation between central screws L_3=121 mm, strip width L_2=1200mm.

2.2 Mesh Generation

The mesh (Fig. 3), built in ANSYS ICEM CFD, is structured and composed of 8.7M of hexahedral cells. The quality of the mesh according to the determinant of the Jacobian matrix (Determinant 3x3x3) is higher than 0.55, having the 90% of the cells a determinant higher than 0.9. The minimum internal angle of each element is higher than 18 degrees and the thickness of the first cell on strip is 0.6 mm.

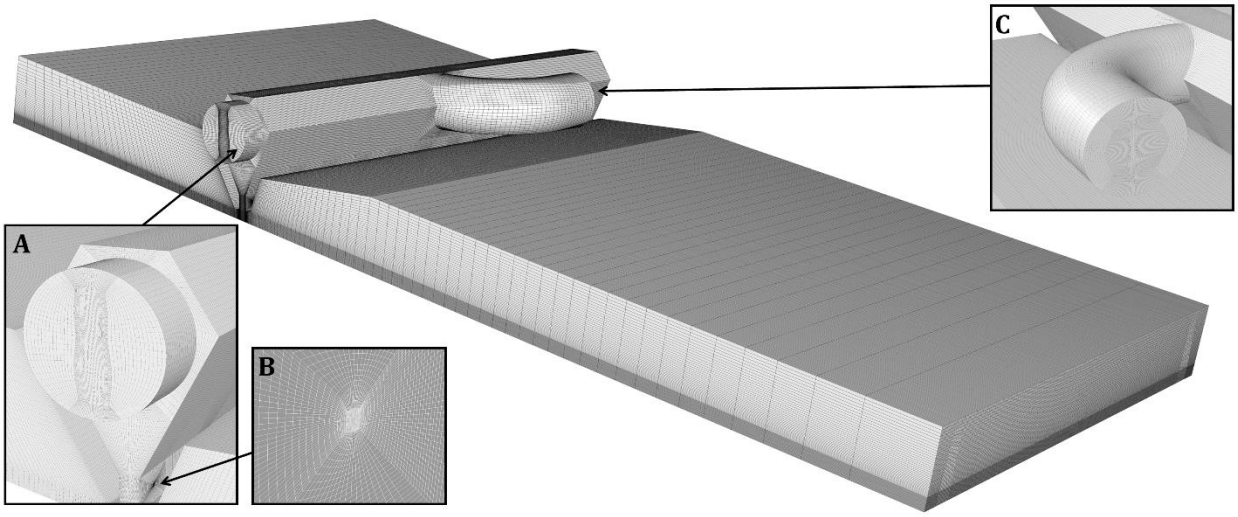

Fig. 3. Mesh detail. A) Lateral feeding, B) Mesh around the screws, C) Central feeding

2.3 Numerical Model

The simulation of the model was made in ANSYS FLUENT 16, which uses the finite volume method to solve the Navier-Stoke equations. The model is incompressible since the Mach number (equation (1)) at the nozzle outlet is about 0.1.

$$Ma = \frac{v}{c} \quad (1)$$

Thus, the Navier-Stokes equations to be solved considering the assumption of incompressible flow are:

$$\frac{\partial u_i}{\partial x_i} = 0 \quad (2)$$

$$\frac{\partial u_i}{\partial t} + \frac{\partial u_j u_i}{\partial x_j} = \frac{\partial}{\partial x_j}\left(\mu \frac{\partial u_i}{\partial x_j}\right) - \frac{1}{\rho}\frac{\partial p}{\partial x_i} \quad (3)$$

The strip is moving at a speed of 600 m/min. The inlet flow of air into the collector, supplied by a "Sonic 350 37.5KW" is 2973 m^3/h. The Reynolds number, which is defined in equation (4), is 57600 according to this numbers.

$$Re = \frac{\rho v L}{\mu} \quad (4)$$

The model system is isothermal, thus the density of the air at 20 ºC is 1.204 kg/m^3 and the kinematic viscosity of the air at 20 ºC is 1.51 x 10^{-5} m^2/s.

Since the blowing conditions and the strip velocity remain fixed in the real process, the simulation was carried out in steady state regime, so the resulted values are an average.

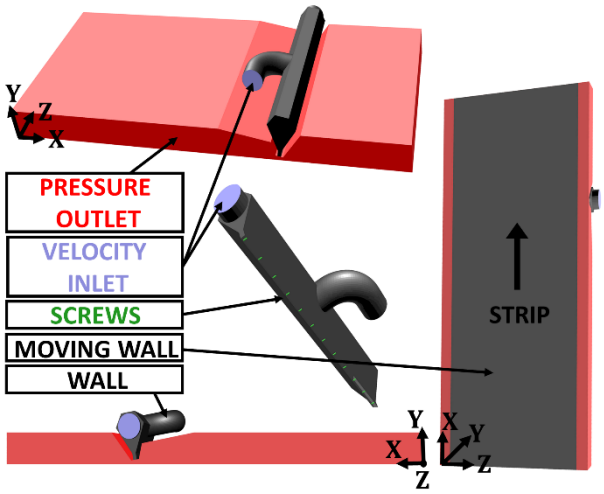

Fig. 4. Boundary conditions of the model

Therefore, the boundary conditions, velocity inlet (45 m/s) and velocity of the strip in the X direction (600 m/min) are constant in every simulation (Fig. 4). Four simulations were performed to evaluate the design of the air-knife collector:

- lateral feeding with screw holes
- lateral feeding without screw holes
- central feeding with screw holes
- central feeding without screw holes.

The velocity-pressure pair was reproduced through a SIMPLE algorithm, a second-order discretization was used for pressure, momentum and turbulent kinetic energy and dissipation rate. The choice of turbulence model has been based on references [20][5] where the Realizable k-ε combined to Enhanced Wall Treatment is recommended. This near wall treatment is appropriate since the y^+ (equation (5)), near the strip is in the required order for the turbulence model being $y^+ \approx 1$.

$$y^+ = \frac{y u_t}{\nu} \quad (5)$$

2.4 Mesh sensitivity and validation

It is known that the mesh resolution plays a critical role in these CFD simulations because it is important to faithfully reproduce the jet shear layer. Prior to perform the CFD simulations, a simple 2D geometry without screws holes and with the planar jet impinging perpendicularly onto a static plate, the same case as [14], was created in order to validate the numerical model and analyze the mesh independency.

Three meshes were generated, considering the necessity of cells in the vicinity of the jet, from course to dense to ensure that the result from the simulations were sufficiently mesh-independent (Fig. 5).

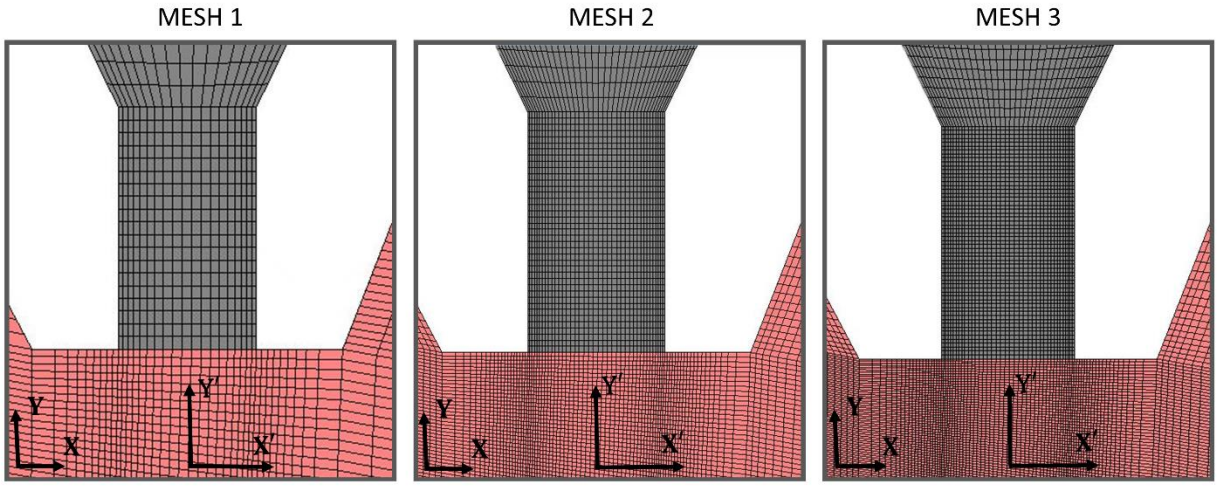

Fig. 5. Detail of the mesh in the vicinity of the impingement. Perpendicular jet impingement.

It was compared the pressure against the length into the impinging line, as it was made by previous authors [14], who studied the pressure field against *X/D* for various *H/D*. According to the manufacturers guidelines for installing these devices, the ratio should be *H/D*≈1. The author [14] uses a Reynolds number of 11000, and the model that is being studied has a Reynolds number approximately 5 times higher. Despite the fact that many authors defend the independence of the impingement pressure on Reynolds number [14][22], it was decided to analyze the influence of *Re* by simulating the

same case as [14]. As can be seen in the Fig. 6, the difference of the Reynolds number is negligible. It is important to remark that the impingement pressure distribution shown by the authors differed from the others in the *x/D* direction in an average of 7%. This fact might be due to the geometry of the gap of the nozzle. Furthermore, all of them follow the same tendency. The mesh 1 has a worse prediction than the other two, whereas the higher the mesh size, the lower the differences between meshes. According to this sensitivity analysis the mesh selected to perform the simulations is the mesh 2 because it offers results that differ from the experimental below 0.2% with a lower computational cost than the mesh 3.

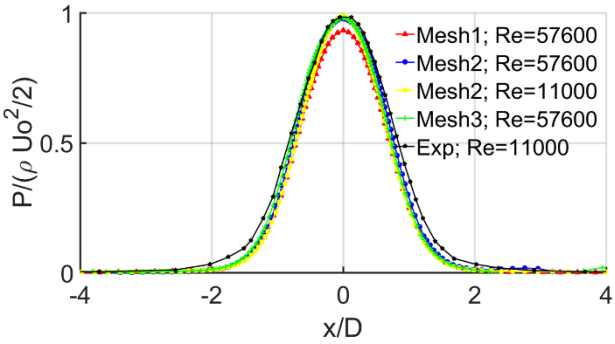

Fig. 6. Mesh Independence and validation. Experimental data (in black) was taken from [14].

It is important to note that the 3D model created with the aim of performing the numerical analysis of the whole air knife reproduces exactly the 2D meshing of the validation in the jet region.

3. Results and discussions

In order to evaluate the performance of the different configurations of the air-knife, having a wider view of the phenomena, velocity and pressure values were extracted from the model. First, as a general view of the problem, it can be seen a different flow distribution within the collector. Fig. 7 shows the velocity streamlines for both configurations: central and lateral feeding. It can be concluded that the central feeding has, in general, a less uniform distribution than the lateral feeding, but lateral feeding has a weak point in the side where the feeding is connected. This defect at the feeding side in the lateral feeding arrangement, which will be shown later thoroughly, could lead into a lack of flow in this side of the air knife. This would involve a non-satisfactory wiping of the liquid.

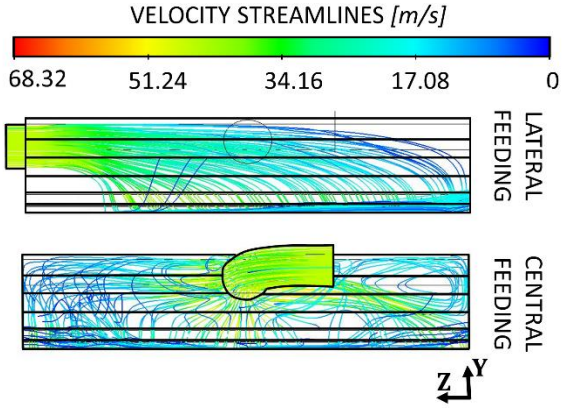

Fig. 7. Velocity Streamlines for central/lateral feeding air-knife without screws.

Fig. 8 corresponds to a plane at *Z*=0.6 m, just in the middle of the air-knife at the same point of the central feeding. In this plane, static pressure and velocity magnitude contours are plotted for the two configurations with the aim of analyzing the effect of the central feeding on the nearest region where the lateral feeding provides a uniform patter as is shown in Fig. 7. Therefore, on the left, the lateral feeding collector shows a typical pressure and velocity distribution of an impinging jet, having a uniform pressure inside the collector and reaching the maximum velocity at the outlet of the air knife.

Regarding central feeding, a clear pressure gradient is observed in the pressure contours (Fig. 8), being associated with a large flow detachment just below the feeding inlet. The magnitude of this flow detachment can also be seen in the velocity contour of central feeding plot (Fig. 8). Hence, a great amount of loss is generated in this region so the jet at the outlet is affected as well. In the velocity contour of central feeding plot (Fig. 8), looking at the outlet of the air knife, the nozzle is partially blocked in this region due to the vortex created at the collector inlet. Therefore, the jet coming out from the nozzle towards the strip is narrower, and its maximum velocity is larger than in the lateral feeding configuration. It can be seen in the pressure contour of the central feeding plot (Fig. 8) that the stagnation region is smaller and slightly displaced because of this effect. Although the purpose of this figure is not the Wall Jet generation on the strip, it is clearly seen that the larger stagnation region in the lateral feeding causes a more uniform wall jet downstream the impingement.

The 3D effects created by the feeding type can be seen in the next figures (Fig. 9, Fig. 10 and Fig. 11).

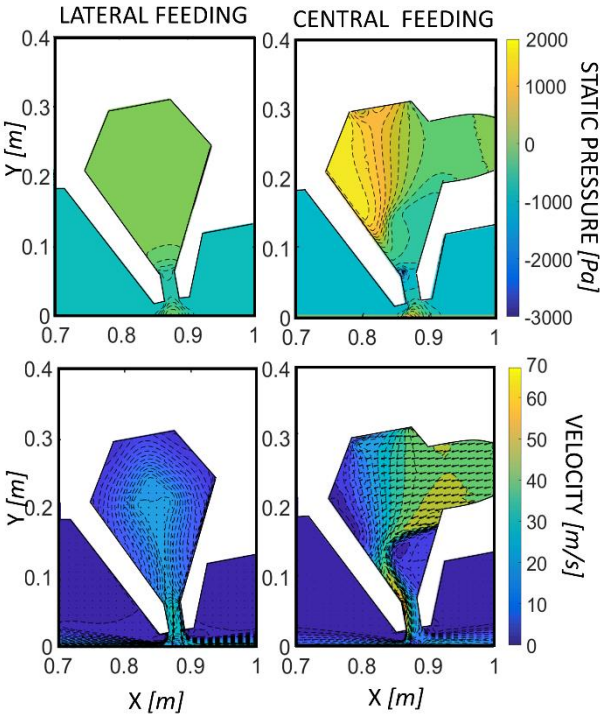

Fig. 8. Velocity and Static Pressure of a transversal plane of the air-knife for central/lateral feeding without screws at Z=0.6m.

The magnitude of the Y' velocity in the plane Y'Z (Fig. 1) for the gap between the jet outlet and the strip is shown in Fig. 9, where two phenomena automatically draw in attention:

- Non-uniformity velocity field related with the type of feeding.
- The peaks in the gradients caused by the presence of the screws.

As reflected in Fig. 9, in the case of the central feeding there is a velocity peak at *Z*=0.6 m, that is also shown in Fig. 8. This peak is a consequence of the jet generated at the outlet of the feeding duct.

The influence of the screws is shown as peaks in the contours for both configurations. As it can be seen in Fig. 9, both configurations have strong wakes that are not completely dissipated before reaching the strip. In the lateral feeding collector, the first screw starting from *Z*=1.2 m is not creating wake because it is just below the recirculation zone near the inlet. The screw blocking effect reduces the cross section and thus higher velocities and higher impact pressure, as it will be shown afterwards.

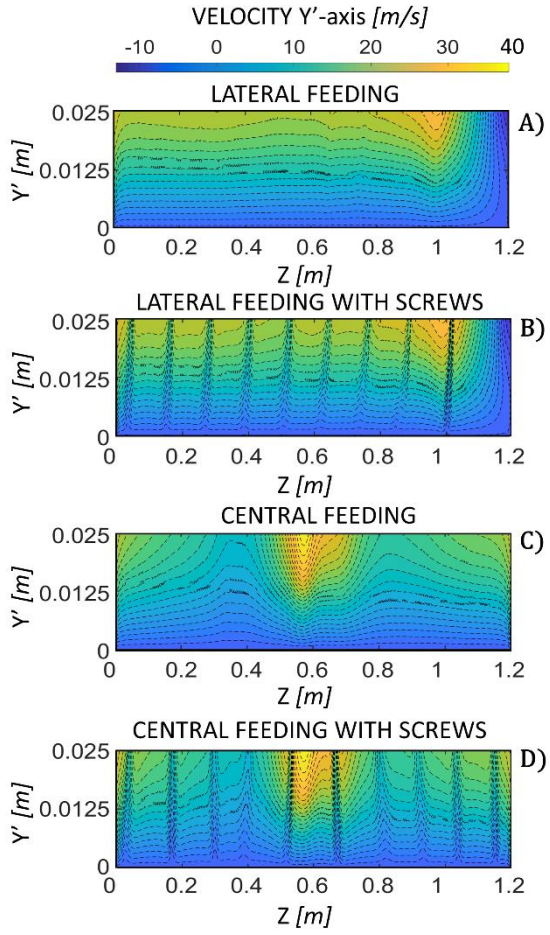

Fig. 9. Velocity contours in Y-axis in the gap between the air-knife and the strip.

The 3D effects previously seen in the velocity field will affect the stagnation region on the strip. In order to analyze this effect, the static pressure (*P*) was taken from the strip surface at the jet impinging line (Fig. 2) for all the different configurations of the collector: lateral feeding with/without screws and central feeding with/without screws (Fig. 10).

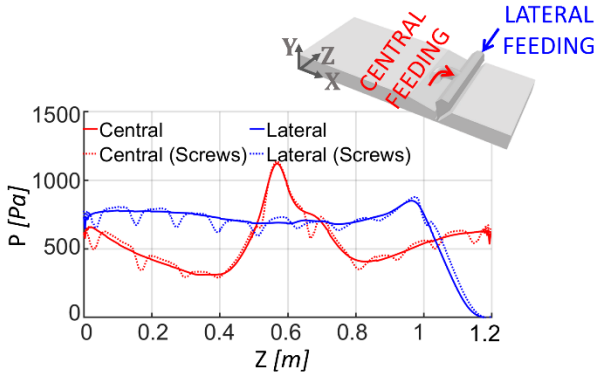

Fig. 10. Static Pressure [Pa] along jet impinging line.

At first sight, it can be extracted from Fig. 10 that the performance of the air knife depends critically on the position of the feeding line. The static pressure in the case of central feeding configuration is not uniform while lateral feeding configuration is approximately uniform in most of the span except just close to the inlet.

Central feeding creates a larger impingement pressure,

above 1kPa, just in the middle of the strip whereas a lack of pressure is detected in lower *Z*-coordinates, reaching a value of 311Pa. At larger *Z*-coordinates the pressure reaches average values remaining approximately constant between *Z*=0.8m and Z=1.2m, being larger than the values at *Z*<0.6m. This lack of symmetry in *Z*-coordinate with respect to the inlet, is produced by the elbow (see Fig. 3-C). The curvature of the pressure gradient created at the elbow drives the flow towards *Z*>0.6m when entry into the collector, producing higher velocities in this region. This is caused by the position of the elbow of the feeding duct, which is too short to suppress all the Z-velocity of the incoming flow.

On the other hand, lateral feeding shows a completely different pattern. The impingement pressure remains constant along almost the whole width of the strip, from *Z*=0 to *Z*=1 (Fig. 10). However, this configuration fails to maintain a minimum pressure in the feeding side. This point is undoubtedly a bottleneck in the wiping process.

Apart from the differences depending on the feeding, the presence of the screws can be easily detected because the data show a clear influence of the wakes on the impingement pressure. This effect is seen for both configurations, central and lateral feeding. Considering the peaks produced by the screws (Fig. 10) the effect of the impinging pressure is reduced by 30%.

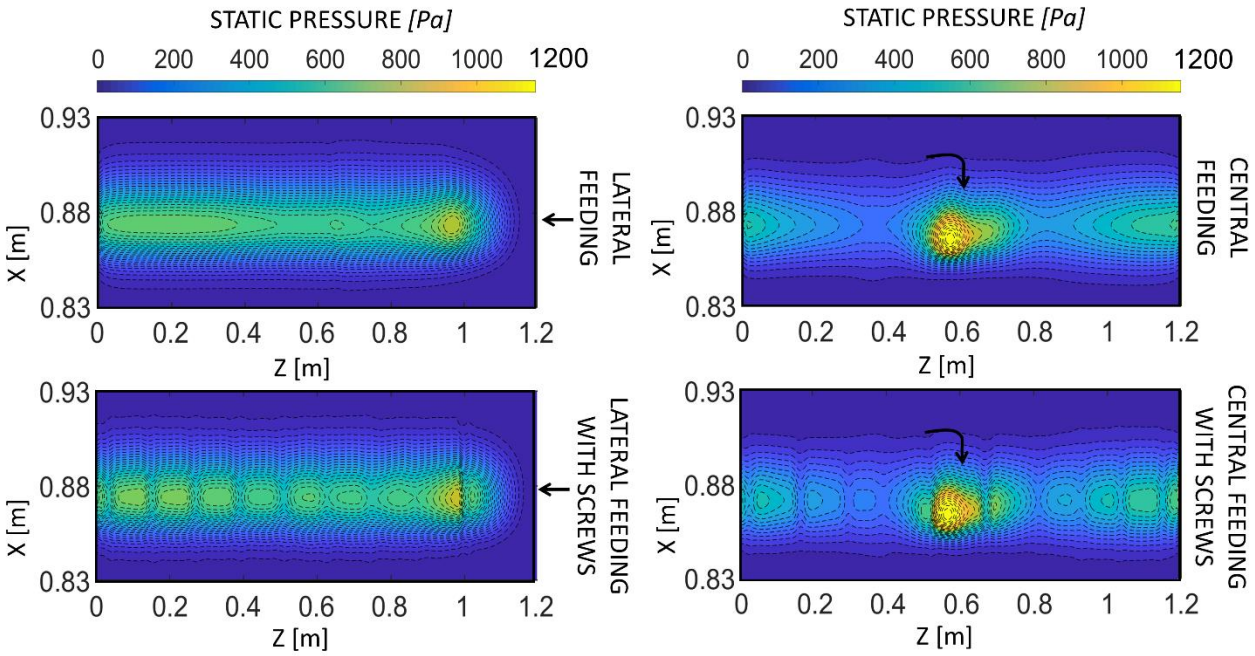

Fig. 11. Static Pressure contours on the strip where the influence of the screws can be seen.

In the Fig. 11, it is presented the static pressure contours on the strip around the stagnation line. In the lateral feeding configuration, an average pressure of 750 Pa can be seen in a uniform width above 0.032m while in the central feeding configuration it is presented a peak of pressure at *Z*=0.6m and an average pressure of 600Pa in a width of 0.023m located at *Z*>0.6m.

Although there is certain dependency on the position of the screw, most screw effects are the same. The relative position of the screws with respect to the feeding duct determines the wake direction. Regarding lateral feeding, they are equally spaced and there is no wake in *Z*>1.2m due to the absence of flow. In the case of central feeding, they are projected in different directions due to the irregular flow pattern that was seen in Fig. 7. These facts can be seen in Fig. 12 where it is compared the velocity contours in the plane Y'-Z for both configuration: central and lateral feeding, with screws.

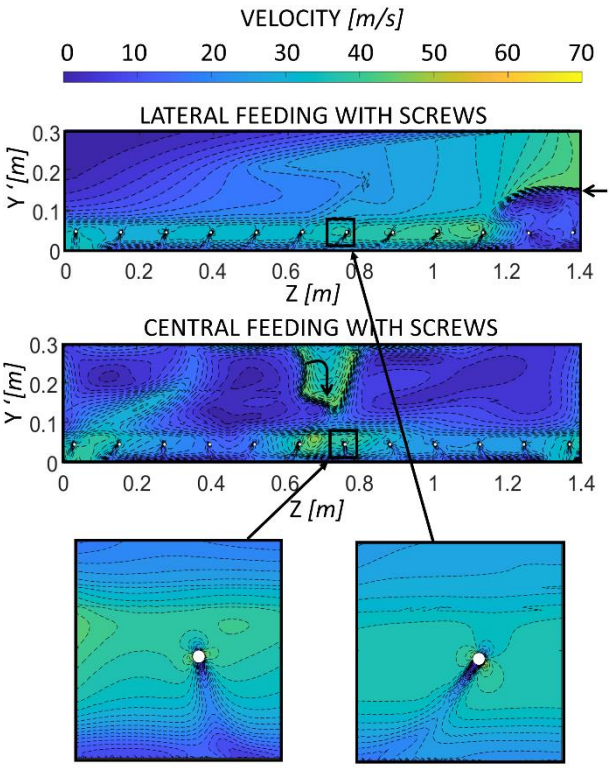

Fig. 12. Velocity contours in Y'Z plane for lateral/central feeding with screws.

In addition to that, the TKE (Turbulent Kinetic Energy) is analyzed in the central feeding with screws case. As can be seen in Fig. 13, there is a high turbulent zone coinciding with the central space of the air-knife (approximately at *Z*=0.9, caused by the type of feeding. This turbulent flow leads to notable fluctuations. This pattern of TKE is not seen in the lateral feeding case.

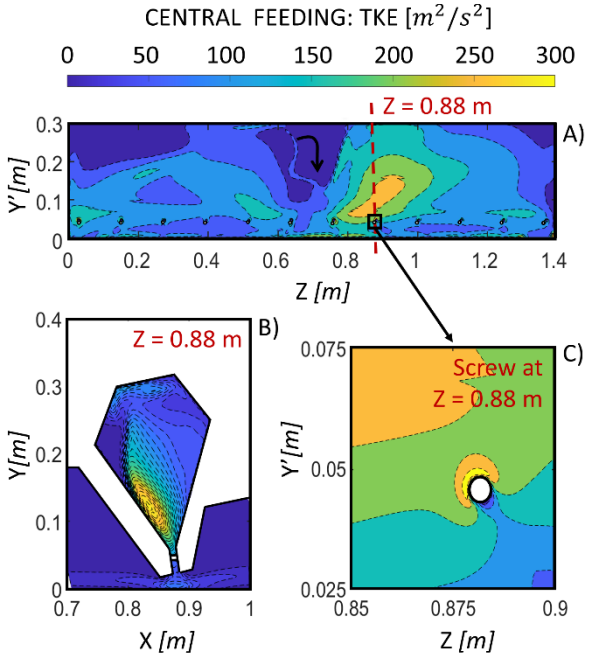

Fig. 13. TKE (Turbulent Kinetic Energy) contours for central feeding case with screws. A) Y'Z plane of the complete air-knife. B) YX plane at Z=0.88 m (coinciding with one of the screws). C) Zoom view of the Y'Z plane for the screw at Z=0.88 m.

Moreover, in Fig. 13, C, the TKE for the screw at *Z*=0.88 m is shown.

In the Fig. 15, wall shear stress distribution on the strip surface is shown. As expected, the shape of the wall stress distribution that is created by the wall jet, depends on each different geometry that were analyzed in this work. For no-slip wall conditions, FLUENT uses the properties of the flow adjacent to the wall boundary to predict the shear stress on the fluid at the wall. As it can be seen, there is a difference on the wall shear stress contour along the *Z*-axis due to the different type of feeding. In the case of lateral feeding, it can be concluded that in *Z*=1-1.2 m there is a conflictive point where the wiping is not as effective as in the rest of the strip. This can lead to water passing through the air knife in this side of the strip.

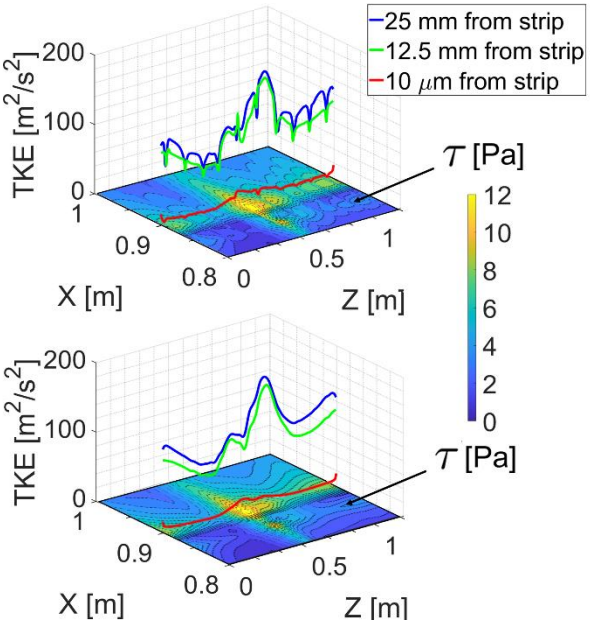

Fig. 14. Relation between TKE of the jet and Wall Shear Stress comparing both cases of central feeding with and without screws.

On the other hand, it was previously seen (Fig. 11) that central feeding has its weak point in *Z*=0.2-0.4 m. This region could become a sink which would create a problem allowing patches of water passing through the air knife. The screw influence in the shear stress is not significant but it can be appreciated more unstable lines of TKE in the case of the geometry with screws (Fig. 14), that have an influence in the Wall Shear Stress. Nevertheless, the effect of the TKE is dissipated when it is closer to the strip.

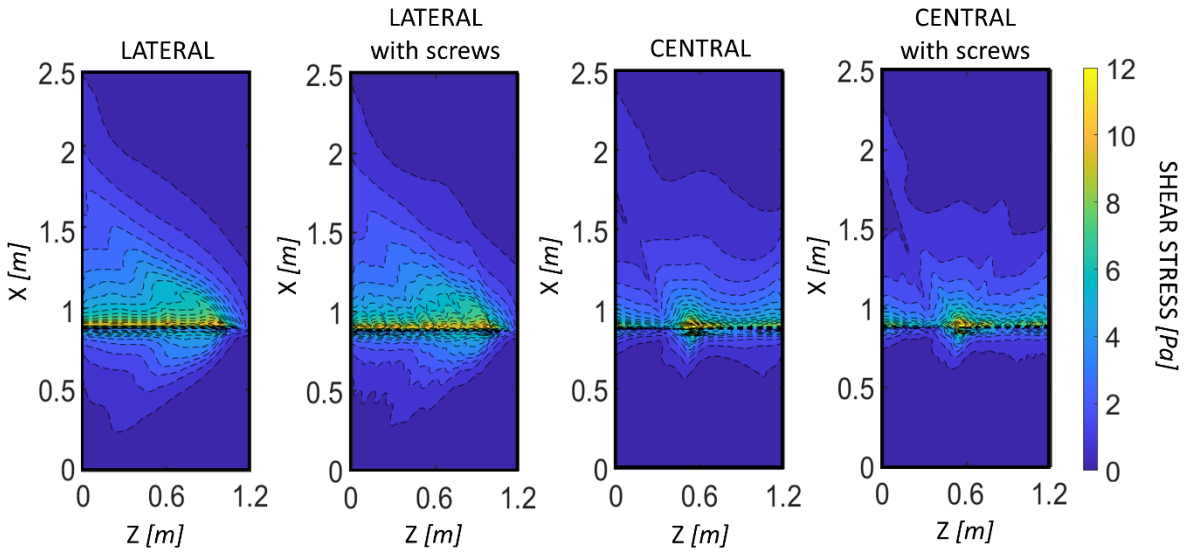

Fig. 15. Shear Stress on the strip surface.

3. Conclusions

In this work, two different configurations of commercial air-knives were simulated in a numerical model created in a commercial software ANSYS Fluent v16, to analyze the aerodynamic performance of each configuration. The numerical model was validated with experimental data taken from the bibliography.

The disorder of the flow created at the entrance of the collector is critical in its performance, being higher in the case of the central feeding case. This fact is related with many losses and with a non-uniform velocity pattern at the outlet. On the other hand, in the case of the lateral feeding collector, despite having a more uniform pattern, there is a whirl that generates a weak point in the side of the lateral feeding.

Besides, the central feeding geometry has a point of large impingement pressure in the middle of the collector, coinciding with the feeding position, and a lack of pressure in lower Z-coordinates due to the elbow of the pipeline. Nevertheless, the central feeding geometry manage to achieve a more uniform wall jet which results in a better wiping distribution in terms of the whole strip width. In contrast, in the lateral feeding, the weak point could lead to let the water going through the side of the strip, but this problem can be fixed by making the collector larger so that the feeding of the collector could be more separated from the strip side.

In addition, it is proved that the screws used to assess the continuous width of the nozzle of the air-knife have a negative influence in the impinging pressure, since the wake downstream the screws reach the strip surface. However, this effect is less important than the effect of the feeding.

The results obtained show that the performance of a single air-knife would result in an unsatisfactory liquid removal. Changes in the arrangement of the device, such as the blowing distance, the air-knife inclination, the nozzle width, multi-lateral feeding or even the combination of several air-knives, could cause an improved performance of the wiping system. Therefore, future works should be focused on analyzing the effect of this variables.

Acknowledgments

C.M.-G. is supported by the Spanish “Ministerio de Educación Cultura y Deporte” within the “Doctorados Industriales” Program (grant number DI-17-09596)

M.G.-D. is supported by the Spanish “Ministerio de Educación, Cultura y Deporte” within the “FPU” Program (grant number FPU15/04375)

Nomenclature

–

Ma : Mach number
L : Characteristic linear dimension
Re : Reynolds number
v : Flow velocity [m·s^{-1}]
c : Speed of sound in the medium [m·s^{-1}]
v_t : Friction velocity [m·s^{-1}]
y^+ : Dimensionless wall distance
y : Absolute distance from the wall
ρ : Density of the fluid [kg·m^{-3}]
μ : Dynamic viscosity of the fluid [Pa·s]
ν : Kinematic viscosity of the fluid [$m^2 \cdot s^{-1}$]

References

[1] A. S. Mujumdar, “Research and Development in Drying : Recent Trends and Future Prospects,” *Dry. Technol. An Int. J.*, vol. 22: 1–2, pp. 1–26, 2004, doi: 10.1081/DRT-120028201.

[2] British Steel Coorporation, “Air Nozzles Wipe Away Steel Rolling Problem,” *Materials and Design*, vol. 8, no. 4, p. 237, 1987.

[3] H. Yadav and A. Agrawal, “Self-Similar Behavior of Turbulent Impinging Jet Based upon Outer Scaling and Dynamics of Secondary Peak in Heat Transfer,” *Int. J. Heat Fluid Flow*, vol. 72, pp. 123–142, 2018, doi:

10.1016/j.ijheatfluidflow.2018.06.001.

[4] S. Yao, Y. Guo, N. Jiang, and J. Liu, "International Journal of Heat and Mass Transfer An experimental study of a turbulent jet impinging on a flat surface," *Int. J. Heat Mass Transf.*, vol. 83, pp. 820–832, 2015, doi: 10.1016/j.ijheatmasstransfer.2014.12.026.

[5] D. Muñoz-Esparza, J. M. Buchlin, K. Myrillas, and R. Berger, "Numerical investigation of impinging gas jets onto deformable liquid layers," *Appl. Math. Model.*, vol. 36, no. 6, pp. 2687–2700, 2012, doi: 10.1016/j.apm.2011.09.052.

[6] P. Fillingham and I. V Novosselov, "Wall jet similarity of impinging planar underexpanded jets," *Int. J. Heat Fluid Flow*, vol. 81, no. December 2019, p. 108516, 2020, doi: 10.1016/j.ijheatfluidflow.2019.108516.

[7] Robert D. Blevins, *Applied Fluid Dynamics Handbook*. 1984.

[8] C.V. Tu; J.D. Hooper; D.H. Wood., "Wall pressure and shear stress measurements for normal jet impingement.pdf," in *11th Australian Fluid Mechanics Conference*, 1992, pp. 1109–1112.

[9] S. Beltaos, "Oblique Impingement Of Circular Turbulent Jets," *J. Hydraul. Res.*, pp. 37–41, 2010, doi: 10.1080/00221687609499685.

[10] H. Y. Hwang and G. A. Irons, "A water model study of impinging gas jets on liquid surfaces," *Metall. Mater. Trans. B Process Metall. Mater. Process. Sci.*, vol. 43, no. 2, pp. 302–315, 2012, doi: 10.1007/s11663-011-9613-3.

[11] K. Myrillas, A. Gosset, P. Rambaud, and J. M. Buchlin, "CFD simulation of gas-jet wiping process," *Eur. Phys. J.*, vol. 97, pp. 93–97, 2009, doi: 10.1140/epjst/e2009-00885-y.

[12] C. Pfeiler, W. Eßl, G. Reiss, C. K. Riener, G. Angeli, and A. Kharicha, "Investigation of the Gas-Jet Wiping Process − Two-Phase Large Eddy Simulations Elucidate Impingement Dynamics and Wave Formation on Zinc Coatings," *Steel Res. Int.*, vol. 88, no. 9, pp. 1–10, 2017, doi: 10.1002/srin.201600507.

[13] E. A. Elsaadawy, G. S. Hanumanth, A. K. S. Balthazaar, J. R. McDermid, A. N. Hrymak, and J. F. Forbes, "Coating weight model for the continuous hot-dip galvanizing process," *Metall. Mater. Trans. B Process Metall. Mater. Process. Sci.*, vol. 38, no. 3, pp. 413–424, 2007, doi: 10.1007/s11663-007-9037-2.

[14] C. V. Tu and D. H. Wood, "Wall pressure and shear stress measurements beneath an impinging jet," *Exp. Therm. Fluid Sci.*, vol. 13, no. 4, pp. 364–373, 1996, doi: 10.1016/S0894-1777(96)00093-3.

[15] C. H. Ellen and C. V. Tu, "An Analysis of Jet Stripping of Molten Metallic Coatings.pdf," in *Eighth Australasian Fluid Mechanics Conference*, 1983, pp. 2C.4-2C.7.

[16] J. A. Thornton and H. F. Graff, "An analytical description of the jet finishing process for hot-dip metallic coatings on strip," *Metall. Trans. B*, vol. 7, no. 4, pp. 607–618, 1976, doi: 10.1007/BF02698594.

[17] H. G. Yoon, G. J. Ahn, M. K. Chung, and J. K. Kim, "Aerodynamic Investigation of Air Knife System to Find Out the Mechanism of the Check Mark in a Continuous Hot-Dip Galvanizing Process," in *International Mechanical Enginnering Congress and Exposition*, 2008, pp. 1–7.

[18] A. Gosset, D. Lacanette, S. Vincent, E. Arquis, J. M. Buchlin, and P. Gardin, "LES – VOF simulation of gas-jet wiping : confrontation to experiments," 2005.

[19] H. So, H. G. Yoon, and M. K. Chung, "CFD Analysis of Sag Line Formation on the Zinc-coated Steel Strip after the Gas-jet Wiping in the Continuous Hot-dip Galvanizing Process," vol. 51, no. 1, pp. 115–123, 2011.

[20] A. Gosset, P. Rambaud, L. Castellano, M. Dubois, and J. M. Buchlin, "Modeling of gas-jet wiping at small standoff distances," *Sixth Eur. Coat. Symp.*, 2005.

[21] P. Naphade, A. Mukhopadhyay, and S. Chakrabarti, "Mathematical Modelling of Jet Finishing Process for Hot-dip Zinc Coatings on Steel Strip," *ISIJ Int.*, vol. 45, no. 2, pp. 209–213, 2005, doi: 10.2355/isijinternational.45.209.

[22] E. Baydar and Y. Ozmen, "An experimental and numerical investigation on a confined impinging air jet at high Reynolds numbers," *Appl. Therm. Eng.*, vol. 25, pp. 409–421, 2005, doi: 10.1016/j.applthermaleng.2004.05.016.

Author information

Celia Miguel-González studied Mechanical Engineering in Oviedo University. Nowadays, she is a Ph.D student supported by the Spanish "Doctorados Industriales" Program. Her research interests are related with drying systems in steel manufacturing.